BJET
(Bayero Journal of Engineering and Technology)
https://bjet.ng/index.php/jet

Research Article
2026, Vol. 21 (2), 87-95

EVALUATION OF TENSILE AND FATIGUE BEHAVIOURS OF NOVEL A356/MELON HUSK ASH NANOCOMPOSITE

Usman, I.[1], Abdulwahab, M.[2], Ause, T.[3], Bello, K.A.[4]

[1,2,3,4]Department of Metallurgical and Materials Engineering, Ahmadu Bello University, Zaria, Nigeria
[2]Department of Metallurgical and Materials Engineering, Air Force Institute of Technology, Kaduna, Nigeria

*Corresponding author email: iusman@abu.edu.ng

Received: 23-03-2026
Revised: 01-06-2026
Accepted: 22-06-2026
Published: 24-06-2026

Abstract: *Lightweight materials such as aluminum matrix composites are gaining prominence in automobile manufacturing due to their competitive properties, with further improvement in properties is achievable by exploiting nanotechnology and developing nanocomposites. The present study explores the tensile and fatigue behaviours of a novel lightweight aluminium-based nanocomposite—A356 reinforced with melon husk ash nanoparticles (MHAnp). Melon husk ash nanoparticles (MHAnp) produced from an abundant Nigerian agro-waste, Egusi melon (Citrullus colocynthis L.) husks, were used to fabricate an A356/MHAnp composite through a modified stir-casting route, i.e., a low-frequency vibration-assisted stir casting. Samples cast were evaluated for tensile and fatigue performance using standard test procedures. X-ray diffraction (XRD) and optical microscopy (OPM) and scanning electron microscopy (SEM) were used to study the microstructure of the fabricated samples and morphology of the fatigue-fractured surfaces, respectively. XRD patterns of the nanocomposite revealed presence of α-Al, Si, β-Al_5FeSi and SiO_2, while optical micrographs of the samples showed a refined microstructure of primary α-Al dendrites, acicular Si and a relatively even distribution of nanoparticles. Results of tensile tests showed that the nanocomposite exhibited improved properties over the as-cast aluminium alloy. The improvements are by 22.85, 3.09 and 8.00 % for tensile strength, yield strength and ductility, respectively. Compared to the as-cast aluminium alloy sample, the nanocomposite sample exhibited a 3.12% improvement in fatigue strength and 10.60% improvement in fatigue life. Fractography of fatigue-fractured samples using SEM indicated that, despite low-frequency vibration during processing, some nanoparticle agglomeration persisted, contributing to crack initiation. In summary, this study demonstrates that melon husk ash nanoparticles are a viable and effective reinforcement for aluminium matrix composites, offering a sustainable pathway to enhance mechanical and fatigue properties for lightweight automotive applications.*

Key words: A356 aluminium alloy; Nanocomposite; Fatigue; Tensile properties; Melon Husk Ash

1 Introduction

Aluminum alloys reinforced with various reinforcement materials, universally known as aluminum matrix composites (AMCs) have been the subject of research for more than three decades owing to their superior properties. Replacing conventional monolithic aluminum alloys because of their failure to meet the ever evolving demand for high performance in many applications, AMCs have the right combination of properties such as higher stiffness, superior strength, improved resistance to wear and low coefficient of thermal expansion, which magnifies their status as suitable replacement for aluminum alloys. The utilization of AMCs in various industries

including aerospace, automotive, marine and nuclear is now commonplace (Moses *et al.*, 2016; Ba and Sun., 2021). A wide range of carbide, oxide, boride and nitride particles have been used as particulate reinforcements to produce AMCs. Introducing the hard particles into soft aluminium matrices improves their mechanical properties. However, synthesizing these ceramic materials is neither economical nor environmentally friendly. Taking all of these into consideration, researchers have found great potential in agro-waste based reinforcements due to their economic viability and abundance availability (Parveez *et al.*, 2021). In addition, since these materials are frequently disposed in an open land resulting in environmental contamination, converting them to reinforcement materials will not only cutting down cost of production of composite materials but also solve the problem of solid waste management. Agro-waste materials such as rice husk ash (RHA), groundnut shell ash (GSA), coconut shell ash (CSA), melon shell ash (MSA) have been utilized by the researchers as reinforcing materials for improving the properties of AMC's (Lancaster *et al*., 2013; Parveez *et al*., 2021). In these composites, deleterious reactions at matrix-reinforcement are avoided due to the presence of oxides in the materials, unlike in some systems involving synthetic ceramic reinforcements such as SiC where formation of Al_4C is highly probable if adequate measures are not taken (Parveez *et al*., 2021).

Improved strength is usually obtained for Al alloys reinforced with micron-sized materials compared with the unreinforced aluminum alloys, however, a significantly reduced ductility limits their widespread applications. Thus aluminum matrix nanocomposites (AMNCs) has evolved to overcome the poor ductility of AMCs (Mousavian *et al.*, 2016). Incorporating nano-reinforcements in AMCs significantly enhances their mechanical properties, particularly hardness, tensile strength, and compressive strength, while simultaneously retaining the composite's ductility (Sahoo and Das, 2019; Singhal *et al.*, 2025). Fatigue behavior of composites is also significantly influenced by size of the reinforcing particulates. Malaki *et al.* (2020) reported that metal matrices reinforced with fine particles exhibit superior fatigue behavior than those filled with coarse particles, because reducing the size of particles causes an increase in the aspect ratio and a decrease in the inter-particle spacings, thereby allowing strengthening mechanisms such as Orowan to be introduced into the composite. Consequently, the mechanical and fatigue strength of the metal matrix is significantly higher when reinforced with fine particles than when reinforced with coarse particles (Xia *et al.*, 2020; Hassan and Lewandowsky, 2014; Han *et al.*, 1997). However, it is very difficult through stir casting (which is the most widely used and cost-effective composite fabrication route) to uniformly disperse nanosized ceramic particles in molten aluminum alloy due to their large surface-to-volume (Shayan *et al.*, 2020). This has compelled researchers to explore modifications, such as application of ultrasonic vibrations to the molten mixture among several other methods, to improve the viability of the cheap and simple stir casting process (Malaki *et al.*, 2019).

To the authors' best knowledge, there is no report yet on the effect of nano-sized melon husk ash (MHA) on the tensile and fatigue behaviours of aluminum composites, even though positive results have been reported on the effect of micron-sized melon husk ash (MHA) reinforcement on the tensile and tribological properties of some aluminium alloys (Abdulwahab *et al.* 2017; Suleiman *et al.*, 2018 & Abolusoro *et al.,* 2025). Also, several studies, including a study on mechanical properties of A356/SiO_2 nanocomposite fabricated using ultrasonic-assisted casting method by Malaki *et al.* (2022) and study of fatigue behavior of TiO_2 nanoparticles reinforced AA2024 alloy fabricated using stir casting method by Mahan *et al.* (2024) among others, were based on synthetic nano-sized reinforcements. Studies on metal matrix composites reinforced with agro-waste derivative nanoparticles are still scarce. In the present study, therefore, A356/melon husk ash nanocomposite is developed by low-frequency vibration assisted stir casting and the tensile and fatigue behaviours of the developed nanocomposite studied. Aluminum A356 alloy is a hypo-eutectic alloy of the Al-Si system belonging to the 3xx.x series, and one of the widely used casting aluminum alloys in the automotive and aerospace industries (Alam, 2014).

2 Materials and Methods

2.1 Materials

The matrix alloy (A356) is aluminium alloy wheel scraps (AAWS), sourced from an automobile service center located at Zaria, Kaduna State of Nigeria. Chemical composition of the alloy using Optical Emission Spectrometer is shown in Table 1. The Si composition is slightly below that of a standard A356, which is consistent with previous studies on automobile aluminium alloy wheel (Song *et al.* 2012). Melon husk ash nanoparticles (MHAnp) used as reinforcement in this study was synthesized through thermal treatment and mechanical milling. Details of the synthesis route and characterization are reported in

a previous study (Ibrahim *et al.*, 2024). Chemical composition of the MHAnp determined using X-ray florescence spectroscopy shows it is predominantly composed of SiO_2 and the average particle size determined by dynamic light scattering (DLS) analysis is 57.53 nm as shown in Table 2 and Figure 1, respectively.

Table 1: Chemical composition of aluminium alloy wheel scraps (AAWS)

Element	Weight %
Al	91.87
Si	6.22
Mg	0.33
Cu	0.02
Fe	0.27
Mn	0.03
Sr	0.01
Others	Balance

Table 2: Chemical composition of melon husk ash nanoparticles (MHAnp)

Composition	Weight %
SiO_2	39.50
K_2O	8.23
Al_2O_3	8.44
MgO	6.53
CaO	7.66
P_2O_5	15.00
Fe_2O_3	6.09
SO_3	1.70
Na_2O	1.75
SnO_2	1.89
TiO_2	0.92
ZnO	3.90

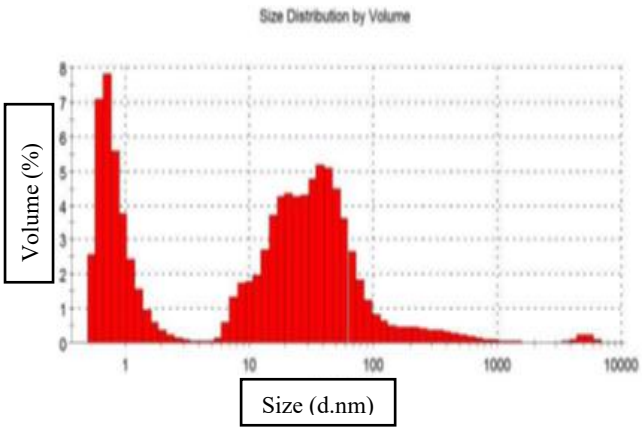

Figure 1: MHA particle size distribution

2.2 Fabrication of A356/MHAnp Nano-Composite

Development of the Al-Mg-Si alloy matrix composites reinforced with 3.5 vol. % melon husk ash nanoparticles (MHAnp) was by stir-casting process. The nanocomposite was fabricated by charging 795g of aluminium alloy wheel scrap (AAWS) pieces into a graphite crucible, heating the charge to a temperature of 800°C and holding at the same temperature for a length of time sufficient for complete melting of the matrix alloy. The temperature of the melt was then lowered to 600°C where it was semi-sold and 3.5 vol. % of MHA nanoparticles (preheated at 350°C for 1 hour) added to it and the mixture stirred continuously at a speed of 400 rpm for 7 minutes. 4 wt. % Mg (with respect to the matrix alloy) wrapped in an Al foil was added to compensate for losses during melting and to improve wettability. The temperature of the melt was then raised to 750°C and the molten mixture agitated for 2 minutes by dipping a probe resonating at a frequency of 60Hz (power output: 150W; voltage: 220V) to improve dispersion of the nanoparticles in the matrix before pouring into a prepared sand mold. A control sample of the aluminum alloy was also produced for comparison of properties.

2.3 Characterization and Testing of Samples

Microstructural examination: To study the morphological features of the as-cast samples, samples of dimensions ø15 x 10 mm cut from the solid cylindrical cast were polished using emery clothes meshed 300, 600, 800, 1200 and 2400, successively. Alumina suspension (0.05 lm) was then subsequently used for final polishing. Thereafter, the samples were submerged in Keller's reagent and etched for 30s. Subsequently, the samples were washed and dried for microstructural observation and capturing under an optical metallurgical microscope equipped with an inbuilt camera (Model No.: NJF:-12A). The microstructures were captured at a magnification of x100. The phases present in the samples were also studied using X-ray diffraction (XRD) analysis.

Tensile test: Tensile test was performed in accordance with ASTM E-8 standard on Electronic Universal Testing Machine (Model: WDW-100KN, S/No.: 190536, made in China). Three standard tensile test samples were machined from each cast sample and tested for tensile properties on the universal testing machine at a crosshead speed of 10cm/min. Average of values for three trials was recorded as tensile strength, yield strength or percent elongation of the sample, as the case may be.

Fatigue analysis: Fatigue test samples were machined according to standard instructions given by ISO 1143:2021.29. Because of the sensitive nature of the test, care was taken in preparing the test samples to avoid scratches and micro-cracks that may serve as crack initiation sites. As-cast A356 alloy and A356/MHA nanocomposite samples. To conduct the fatigue experiments, a rotating fatigue machine, SM-1090 (Model: TQ183418-002, made in China) was used. At least three polished hourglass-shaped samples were fatigued for each stress state. The test was conducted at room temperature and the stress ratio (R) and frequency set at -1 and 50 Hz, respectively. Under the stress-controlled setup, the fatigue test was carried out at five stress levels of 0.3, 0.45, 0.6, 0.75 and 0.9 of yield stress. Applied stresses were converted to equivalent loads using the relationship represented by Equation (1). Considering three times repetitions for each fatigue state, a total of 30 fatigue samples (15 per specimen) were used. The data obtained from the tests were plotted as Applied Stress (S) against mean Number of Cycles to Failure (N) to generate the S-N curve. Analysis of fracture surfaces of the specimens was done using a scanning electron microscope (SEM).

$$F = S\frac{\pi d^3}{32L} \qquad (1)$$

Where F, S, L and d are applied load in N, required test stress in N/mm^2, the force arm length in mm and the specimen diameter in mm, respectively.

3 Results and Discussion

3.1 Microstructural Examination

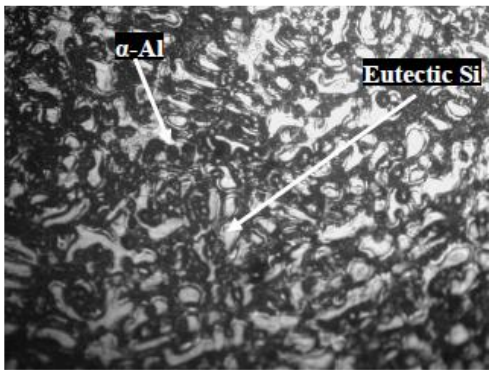

Plate I: Optical micrograph of as-cast A356 alloy at x 100 magnification

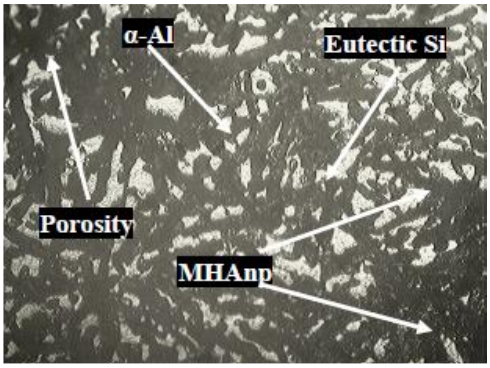

Plate II: Optical micrograph of as-cast A356/MHAnp composite at x 100 magnification

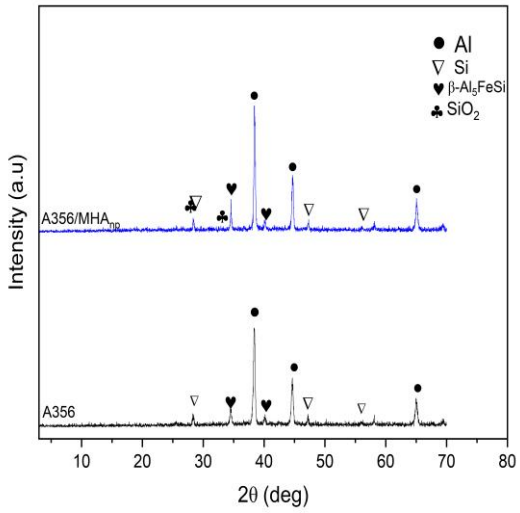

Figure 2: XRD patterns of the samples

The XRD patterns of the samples analyzed using MDI Jade 6 software show the presence of α-Al, Si, β-Al_5FeSi and SiO_2. The XRD spectrum of A356 has the peaks (111) at 2θ= 38.473°, (200) at 2θ = 44.722° and (220) at 2θ = 65.099° corresponding to Al (PDF card no. 99-005); the peaks (111) at 2θ = 28.443°, (220) at 2θ = 47.304° and (311) at 2θ = 56.124° corresponding to Si (PDF card no. 99-0092); and minor peaks (111) at 2θ = 34.594° and (220) at 2θ = 40.165° corresponding to FeSi intermetallic compound , Al_5FeSi (PDF card no. 38-1397). These peaks are common to the other samples, except the peaks (211) at 2θ = 28.794° and (212) at 2θ = 33.127° corresponding to SiO_2 (PDF card no. 47-1300) present in A356/MHAnp which could be from the agro-waste-derived reinforcement— melon husk ash nanoparticles.

The microstructures of the alloy and nanocomposite samples are depicted by the micrographs in Plates I and II, respectively.

Micrograph of the as-cast A356 sample (Plate I) shows a dendritic structure of α-Al and acicular eutectic Si. The micrograph in Plate II, depicting the microstructure of as-cast A356/MHAnp sample, shows finer morphology than that of the alloy, which may have resulted from nanoparticles locking the grain boundaries and preventing excessive grain growth during cooling (Shayan *et al.*, 2020). The microstructure is made up of primary α-Al dendrites, acicular Si and a relatively even distribution of nanoparticles. Some agglomerations are also noticeable at some spots, which may have been the cause for the marginal improvement in some properties (Hoziefa *et al.*, 2016).

3.2 Tensile Properties

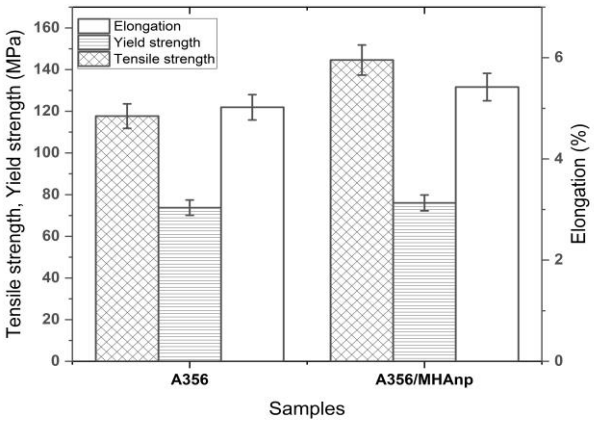

Figure 3: Tensile properties of the samples

Figure 3 shows the tensile properties of the alloy and the nanocomposite samples. The tensile strength values are 117.70 and 144.60 MPa for A356 and A356/MHAnp samples, respectively; the yield strength values are 73.74 and 76.02 MPa for A356 and A356/MHAnp samples, respectively; and the percent elongation values are 5.02 and 5.42 for A356 and A356/MHAnp samples, respectively. The improvement in tensile properties on addition of melon husk nanoparticles can be attributed to the resultant grain refinement and the action of the nanoparticles as barriers to dislocation movement, i.e. Orowan strengthening, thereby overcoming the traditional strength-ductility trade-off and simultaneously improving both properties (Singhal *et al.*, 2025). Similar observations were made by Li *et al.* (2019).

3.3 Fatigue Behaviour

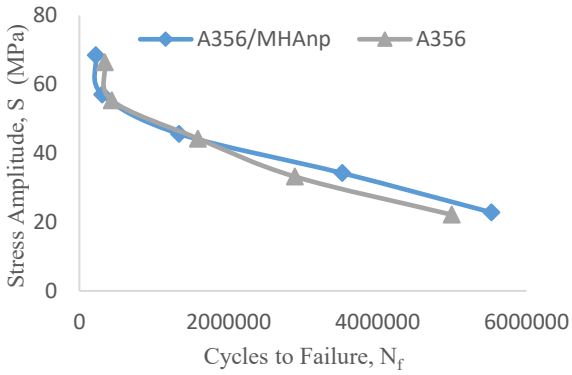

Figure 4: S-N curve of the samples

Fatigue behaviour of the tested samples (A356 alloy and A356/MHAnp) is plotted in Figure 4 as applied stress, S versus number of cycles to failure, N_f. The plots are typical S-N curves, dropping from left to right, characteristic of fatigue behaviour of metallic materials. Within the low cycle fatigue (LCF) region, i.e. $N_f < 1x10^6$, corresponding to high applied stress region— and close to the yield strength of the samples, the alloy sample endured higher number of cycles to failure than the nanocomposite sample. At the highest applied stress level, 0.9 YS, number of cycles to failure are 3.42 x 10^5 and 2.19 x 10^5 for A356 sample and A356/MHAnp sample, respectively. However, this trend changed at lower applied stress levels, i.e., high cycle fatigue (HCF) region, where the nanocomposite sample apparently endured higher number of cycles to failure. At stress level of 0.6 YS, corresponding number of cycles were 2.89 x 10^6 and 3.53 x 10^6 for A356 and A356/MHAnp samples, respectively. In contrast to the LCF region, where applied stress is high—higher than any counter residual stresses in the test sample— and fatigue crack usually initiates at multiple locations, predominantly from the material's free surface where the material can easily deform plastically, crack initiation and propagation in HCF are both critical and characterized by complex phenomena (Malaki *et al.*, 2020). In HCF, the presence of residual stresses in any material is of great significance, because compressive residual stresses can locally reduce the mean stress, therefore limiting the propensity of having regions under micro-plastic cyclic deformation (Salvati, 2024). As a result, the test samples endured higher number of cycles to failure at lower stress levels, and because compressive residual stresses are more in composites than unreinforced alloys in the same condition, they exhibit greater endurance to failure in the HCF region (Mahan *et al.*, 2024). Additionally, there is higher number of grain boundaries in the nanocomposites as a result of grain refinement occasioned by addition of nanoparticles. Due to the refined structure, stress is

distributed evenly throughout the material, aiding in preventing crack growth, and increasing the endurance of composite to failure than the bare alloys (Malaki *et al.*, 2020; Abd-Elaziem *et al.*, 2024). However, none of the tested samples, at the minimum applied stress level of 0.45YS, reached 10^7 cycles or ran out; a phenomenon that could be attributed to the presence of deleterious Al_5FeSi intermetallic compound in the samples. Other factors that may have contributed to the phenomenon are microstructural defects, including agglomeration and pores, in the case of the composite samples (Salvati, 2024). The fatigue strength and corresponding number of cycles to failure of the test samples were determined to be 22.12 MPa (5.00 x 10^6 cycles) and 22.81 MPa (5.53 x 10^6 cycles) for A356 and A356/MHAnp, respectively. Table 3 compares the fatigue properties of the developed composite with that of other nanocomposites developed by other researchers. It is obvious that the novel composite material has great prospects among similar nanocomposite materials for applications involving cyclic loading conditions.

Table 3: Comparison of fatigue properties of the developed nanocomposites and other nanocomposites

Nanocomposite	Processing route	Fatigue strength	Cycles to Failure	Ref.
AA7075/ 9wt%Al_2O_3	Stir casting	62.5	1.4 x10^6	Al-mushedany *et al.* (2022)
A356/ 0.125wt%SiO_2	Ultrasonic assisted-stir casting	25	7.0 x10^6	Malaki *et al.* (2022)
A356/ 3.5vol%MHA	Low frequency assisted stir casting	22.81	5.5x10^6	Present study

3.4 Fractography of Fatigue Fracture Surfaces

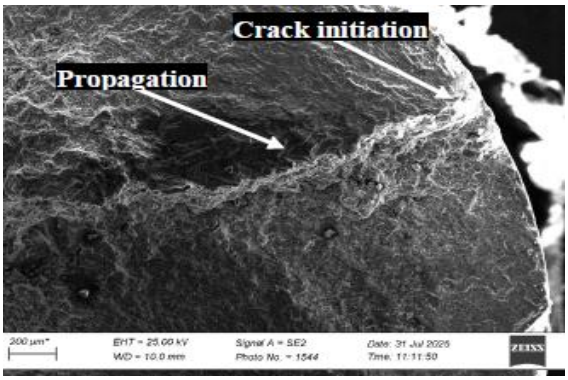

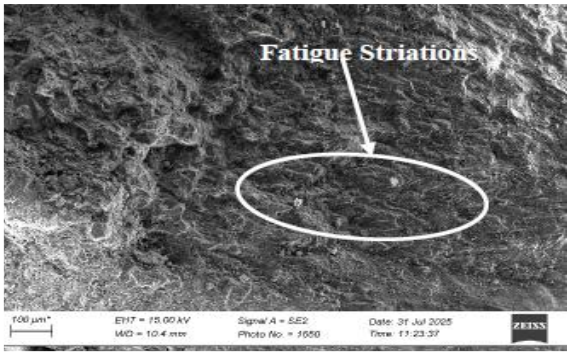

Plate III: Fracture surface of as-cast A356 alloy (a) on a scale of 200µm and (b) on a scale 100µm

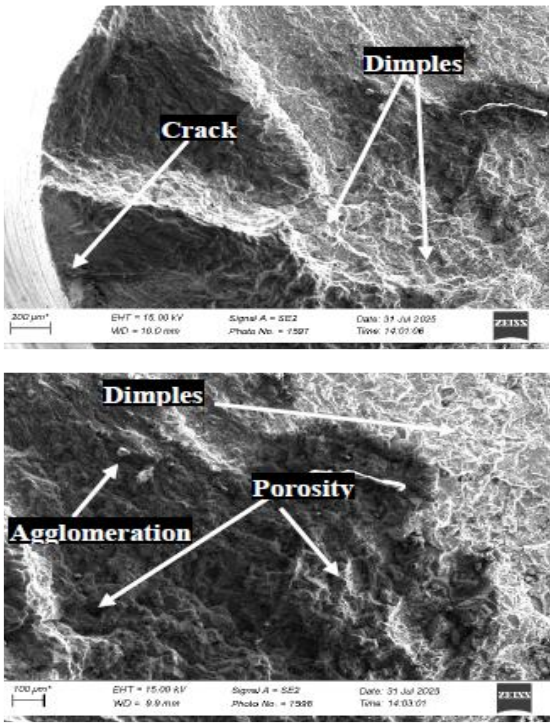

Plate IV: Fracture surface of as-cast A356/MHAnp composite (a) on a scale of 200µm and (b) on a scale 100µm

Fracture surfaces of the fatigue-fractured samples at the lowest test stress levels are shown in Plates III and IV. The surfaces were analyzed using SEM to unravel the mode and cause of fracture of the samples.

In Plates III (a) and (b), the fracture surface of A356 fatigue sample shows microstructural defects that may have contributed to initiation and propagation of cracks. The major defect noticeable is porosity, as shown in Plate III (a). In Plate III (b), fatigue striations showing progression of failure are also obvious. In Plates IV (a) and (b), representing the fracture surface of the as-cast A356/MHAnp composite, fine dimples showing plastic deformation are visible, evidencing the predominant failure mechanism in the nanocomposite is ductile. An advancing crack in the micrograph in Plate IV (a) seems to have been deflected by the reinforcement particle, and because

of the size of the particles, they are not cracked, thereby delaying crack propagation (Myriounis *et al*., 2012; Malaki *et al.*, 2020). The presence of porosity and clusters of MHAnp, however, constituted stress concentration sites in the composite, limiting the number of cycles to failure. These microstructural defects limited the fatigue performance of the composite slightly compared to the findings of other studies on A356 nano-composites, including Malaki *et al.* (2022).

4 Conclusion

A356/melon husk ash nanocomposite has been synthesized through modified stir casting and tensile and fatigue properties of the composite evaluated successfully. From the study, the following conclusions are drawn:

1. The microstructure of as-cast A356/MHAnp sample is composed of a morphology finer than that of the alloy, which may have resulted from nanoparticles locking the grain boundaries and preventing excessive grain growth during cooling.
2. The A356/MHAnp nanocomposite sample exhibited improved tensile properties over the as-cast aluminium alloy sample by 22.85, 3.09 and 8.00 % for tensile strength, yield strength and ductility, respectively. Compared to the as-cast aluminium alloy sample, the nanocomposite sample exhibited a 3.12% improvement in fatigue strength and 10.60% improvement in fatigue life.
3. Fractography of fatigue samples revealed that presence of porosities and clusters of MHA nanoparticles act as stress concentration zones that aided in fatigue failure.
4. Melon husk ash nanoparticles are a viable and effective reinforcement material for aluminium matrix composites, offering a sustainable pathway to enhance mechanical properties for lightweight automotive applications.
5. It is recommended that the nanocomposite be produced through other routes, including ultrasonic-assisted casting, and by optimization of process parameters using response surface methodology (RSM) to optimize the properties of the novel material.

Acknowledgment

The authors acknowledge the support of Department of Metallurgical and Materials Engineering and NLNG Multi-User Lab, both of Faculty of Engineering, Ahmadu Bello University Zaria, Nigeria for providing the necessary facilities and equipment for the research.

References

Abd-Elaziem, W., Khedr, M., Elsheikh, A.H., Liu, J., Zeng, Y., Sabae, T. A., Abd El-Baky, M.A., Darwish, M.A., Daoush, W.M., and Li, X., 2024. Influence of nanoparticles addition on the fatigue failure behaviour of metal matrix composites: comprehensive review. *Engineering Failure Analysis, 155*, p.107751.

Abdulwahab, M., Umaru, O.B., Bawa, M.A., Adams, S.M., and Fatai, S.B., 2017.Wear behavior of Al/15%melon shell ash particulate composite. *Nigerian Research Journal of Engineering and Environmental Sciences, 2*(1), pp.108-114.

Abolusoro, O.P., Khoathane, M.C., and Mhike, W., 2025. Influence of melon shell ash reinforcement on the mechanical and microstructural characteristics of recycled aluminium matrix composites. *Res. Eng. Struct. 11*(2), pp. 783-798.

Alam, M. K. (2014). Thermal and Microstructural Analysis of the A356 Alloy Subjected to High Pressure in the Squeeze Casting (SC) UMSA Technology Platform. Dissertation for Master of Applied Science in Engineering Materials, Department of Mechanical, Automotive & Materials Engineering University of Windsor, Ontario.

Al-Mushehdany, A., Yahya, M.M., Ibrahim, E.K., and Alalkawi, H.J.M. 2022. Nano reinforcement technique as a tool for enhancement of the mechanical and fatigue properties of curved layer, *Struct. 9*, pp. 345–351.

Ba, Y. and Sun, S., 2021. Tensile and fatigue properties of fiber-reinforced metal matrix composites Cf/5056Al, *Composites and Advanced Materials 30*, pp. 1-7.

Han, N.L., Wang, Z.G., and Zhang, G.D., 1997. Effect of reinforcement size on the elevated-temperature tensile properties and low-cycle fatigue behavior of particulate SiC/ Al composites, *Compos. Sci. Technol., 57*, pp.1491–1499.

Hassan, H.A. and Lewandowski, J.J., 2014. Effects of particulate volume fraction on cyclic stress response and fatigue life of AZ91D magnesium alloy metal matrix composites, *Mater. Sci. Eng. A. 600*, pp.188–194.

Hozeifa, W., Toschi, S., Ahmed, M.M.Z., Morri, A.A.A., El-Sayed, S.M.M., El-Mahallawi, I., Ceschini, L., and Atlam, A., 2016. Influence of friction stir processing on the microstructure and mechanical properties of a compocast AA2024-Al_2O_3 nanocomposite. *Materials and Design, 106*, pp. 273-284.

Lancaster, L., Lung, M.H., and Sujan, D., 2013. Utilization of Agro-Industrial waste in metal matrix composites: Towards sustainability. *International Journal of Environmental, Ecological, Geomatics, Earth Science and Engineering, 7*(1), pp. 25-33.

Li, X., Yan, H., Wang, Z-W., Li, N., Liu, J-L., and Nie, Q., 2019. Effect of Heat Treatment on the Microstructure and Mechanical Properties of a Composite Made of Al-Si-Cu-Mg Aluminum Alloy Reinforced with SiC Particles. *Metals, 9,* p.1205.

Mahan, H.M., Konovalov, S.V., Najm, S.M., Mihaela, O., and Trzepieciński, T., 2024. Experimental and Numerical Investigations of the Fatigue Life of AA2024 Aluminium Alloy-Based Nanocomposite Reinforced by TiO_2 Nanoparticles under the Effect of Heat Treatment. *International Journal of Precision Engineering and Manufacturing, 25*, pp.141–153.

Malaki, M., Xu, W., Kasar, A.K., Menezes, P.L., Dieringa, H., Varma, R.S., and Gupta, M., 2019. Advanced Metal Matrix Nanocomposites. *Metal, 9*, p.30.

Malaki, M., Tehrani, A.F., and Niroumand, B., 2020. Fatigue behavior of metal matrix nanocomposites, *Ceram. Int. 46*, pp.23326–23336.

Malaki M., Tehrani A.F. and Niroumand B., 2022. A novel cast nanocomposite with enhanced fatigue life, *JOM*, pp.1–10.

Mani, M. K. (2014). Development of Fe-50Co Alloy and its Composites by Spark Plasma Sintering Doctoral dissertation. Cardiff University, Wales, United Kingdom.

Moses, J.J., Dinahran, I., and Sekhar, S.J., 2016. Prediction of influence of process parameters on tensile strength of AA6061/TiC aluminium matrix composites produced using stir casting. *Trans. Nonferrous Met. Soc. China, 26*, pp.1498-1511.

Mousavian, R.T., Khosroshahi, R.A., Yazdani, S., and Brabazon, D., 2016. Manufacturing of cast A356 matrix composite reinforced with nano- to micrometer-sized SiC particles. *Rare Met.* Doi: 10.1007/s12598-01

Myriounis, D.P., Matikas, T.E., and Hasan, S.T., 2012. Fatigue Behaviour of SiC Particulate-Reinforced A359 Aluminium Matrix Composites. *Strain, 48*, pp. 333-341.

Parveez, B., Maleque, M.A., and Jamal, N.A., 2021. Influence of agro-based reinforcements on the properties of aluminum matrix composites: a systematic review. *J Mater Sci., 56*, pp.16195 – 16222.

Sahoo, B.P., and Das, D., 2019. Critical review on liquid state processing of aluminium based metal matrix nano-composites. *Materials Today: Proceedings, 19*, pp.493-500.

Salvati, E. 2024. Evaluating fatigue onset in metallic materials: Problem, current focus and future perspectives. *International Journal of Fatigue, 188*, p.108487.

Shayan, M., Eghbali, B., and Niroumand, B., 2020. Fabrication of AA2024-TiO_2 nanocomposite through stir casting. *Trans. Nonferrous Met. Soc. China, 30*, pp.2891-2903.

Singhal, V., Shelly, D., Saxena, A., Gupta, R, Verma, V.K., and Jain, A., 2025. Study of the Influence of Nanoparticle Reinforcement on the Mechanical and Tribological Performance of Aluminum Matrix Composites — A Review. *Lubricants, 13*, p.93.

Song, J.Y., Park, J.C., Jeong, B. H., and Ahn, Y.S., 2012. Fatigue behaviour of A356 auminium alloy for automotive wheels. *International journal of Cast Metals Research, 25*(1), pp.26-30.

Suleiman, I.Y., Salihu, & Mohammed, T. A., 2018. Investigation of mechanical, microstructure and wear behaviors of Al-12%Si reinforced with melon shell ash particulates. *The International Journal of Advanced Manufacturing Technology*. Doi: doi.org/10.1007/s00170-018-2157-9

Usman, I., Abdulwahab, M., Ause, T. and Bello, K.A., 2024. Synthesis and charcterization of melon husk ash nanoparticles as potential reinforcement for aluminium matrix

nanocomposites. *Journal of Metallurgical and Materials Engineering* (in press).

Xia, J., Lewandowski, J.J., and Willard, M.A., 2020. Tension and fatigue behavior of Al-2124A/SiC-particulate metal matrix composites, Mater. Sci. Eng. A. 770, p.138518.